



ORIGINAL RESEARCH ARTICLES

OPEN ACCESS

ANALYSIS OF PREDICTIVE CONTROL FOR BOOST CONVERTER IN POWER FACTOR CORRECTION APPLICATION

^{1,*}Nirmala Devi, V. and ²Viswanath Reddy, P.

¹ Assoc. Prof and HOD, Dept of EEE, DR.K.V. Subba Reddy Institute of Technology, Kurnool, AP, India

²PG Scholar, Dept of EEE, DR.K.V.Subba Reddy Institute of Technology, Kurnool, AP, India

ARTICLE INFO

Article History:

Received 29th July, 2017
Received in revised form
14th August, 2017
Accepted 17th September, 2017
Published online 10th October, 2017

Key Words:

Boost Converter,
Power factor correction,
Finite Control Set Model-based
Predictive Control (FCS-MPC),
PI Controller, Current Harmonics.

ABSTRACT

This work presents a boost converter design methodology for active power factor correction, using finite control set model-based predictive control (FCS-MPC) for current control. Moreover, an external proportional integrative (PI) voltage control loop design methodology is explained. This paper also compares the conventional PI current control with MPC current for this application, both in transient load disturbance condition and in steady state different load conditions. The results in rated operation are compared with IEC 61000-3-2 international standard, which establishes limits for current harmonics rms values. The design methodology shows itself effective, with results near to the expected. Both controllers presented advantages and disadvantages, many of them exhaustively discussed in this work

*Corresponding author

Copyright ©2017, Nirmala Devi and Viswanath Reddy. This is an open access article distributed under the Creative Commons Attribution License, which permits unrestricted use, distribution, and reproduction in any medium, provided the original work is properly cited.

Citation: Nirmala Devi, V. and Viswanath Reddy, P. 2017. "Analysis of Predictive Control for Boost Converter in Power Factor Correction Application.", *International Journal of Development Research*, 7, (10), 16095-16107.

INTRODUCTION

A constant preoccupation of industrial equipment producers is to attend international standards on total harmonic distortion (THD) and power factor (PF), specially, in order to sell for markets subjected to standards as IEC 61000-3-2 (1). This norm establishes limits for current harmonic levels in equipment with input current lower than 16 A. The main problem is that industrial and domestic equipment use power converters for developing DC sources or motor drives. The power converters are nonlinear loads which produce distortions in input current distortions that increases the harmonic current levels considerably in the location electrical grid. The high level of harmonic current implies on low power factor, electromagnetic compatibility problems, overload of the electric system, transformer saturation and other issues. One of the worst power converters in terms of THD is the full-bridge monophasic rectifier with capacitive filter (2). A comparative between the norm patterns and the converter (1500 W) is presented in Figure 1. In Figure 1, the need to perform a power factor correction (PFC) in this equipment shows itself obvious. There are two lines of PFC techniques: passive correction and active correction. Passive correction reduces the harmonic content of the input current adding an inductor or a low pass LC filter in the converter input. However, these technique sometimes cannot attend the norm and, when it does, it occurs only near to the rated power of the rectifier. In other hand, active PFC uses a controlled converter to power factor correction. This condition allows high power factor in a large range of operation and still guarantees the correct output voltage, even with disturbances in voltage grid (3), (4).

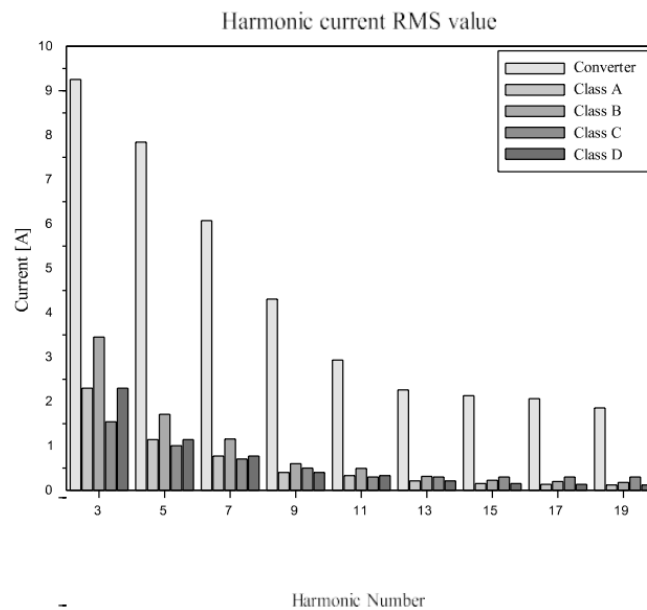


Fig. 1. Harmonic flow of electrons comparative of 1fivezerozero W monophase rectifier and IEC standard

The main converter used for active PFC is the boost DC- DC converter, operating in any conduction mode (continuous, critical or discontinuous) (4). For controlling the converter, usually a proportional- integrative (PI) controller is employed, in a cascade loop configuration. There is an internal and fast current loop and an external and slow voltage loop (3), (4). Recently, many predictive control strategies have been tested for several applications in power electronics, including PFC. The main predictive strategy used in this applications is the finite control set model-based predictive control (FCS-MPC) due to its implementation simplicity, properly developed for power electronics (5). In this technique, there is the treatment of commutation nonlinearity, which makes this technique very attractive. In active PFC with Boost converter, there are, in literature, experimental results of its appliance and validity (6). However, the FCS-MPC has an awful issue for power converters project: the control has variable frequency operation, limited to the half of the sample time (7). It implies on many difficulties to design the passive components of the converter and even to design the external voltage loop. Considering this condition, many works, in active PFC applications have opted for use continuous control set model- based predictive control (CCS-MPC). This predictive strategy models the converter considering a duty cycle as the control action. In the active PFC, there are some works with this control strategy (2), (4), (8)–(10). This work main objective consists in to develop a design method for the boost converter, to apply the FCS-MPC with the maximum current THD reduction and low voltage ripple. The results are compared with the traditional PI controller strategy. In Section II, the FCS-MPC fundamentals are presented. In Section III, the converter and the control design for predictive control technique is shown. In Section IV, the converter and the control design for PI application are made. Simulated results are presented in Section VI. Finally, the conclusions are done in Section VII.

PREDICTIVE CONTROL FUNDAMENTALS

Model-based predictive control was developed in petro- chemical industry in the end of 1970 decade (11). Posteriorly, the research in academy formalized this digital control strategy theory, culminating in several control techniques with the same principles (12). Often, these techniques have some common aspects as the prediction model and the cost function. The prediction model is used to predict the future behavior of the plant, inside a prediction horizon (number of plant future steps predicted). The cost function is used to choose the control action to be applied in the process. The control action is calculated by minimizing the cost function, which weights costs of the system, like tracking errors, control action variation and other parameters (7), (12). For power electronic converters, FCS-MPC can be easily used (5), (13). In this predictive control strategy, treatment of commutation states non linearity is made, considering the future state of all converter switches. In the sequence, a cost function is evaluated. The state which implies lower cost is chosen to be applied to converter switches (5). This technique has the advantage of treating multiple inputs multiple outputs (MIMO) systems, to treat process constraints directly in cost function, without saturation, to do not be dependent of an operation point of the system among others (5).

Prediction Model

Considering a boost converter, for inductor current control, operating in continuous conduction mode (CCM), there are two stages of operation. In the first stage, the switch is active. Thus (3):

$$i[k+1] = i[k] + \frac{t_s}{L} v_{in}[k]. \quad (1)$$

In the second stage, the switch is inactive and $i_L > 0$.

Thus

$$i_L[k+1] = i_L[k] + \frac{t_s}{L}(v_{in}[k] - v_{out}[k]). \quad (2)$$

Thus: Equations (1)-(2) describe the behavior of a future step of the current. It is enough for a FCS-MPC with unitary prediction horizon, which will be used in this work (it means the model is predicted one step in the future). Due to (1)-(2), to evaluate this model, three sensors are necessary: an input voltage sensor (possibly, a resistive divider), an output voltage sensor (similar to previous case) and a current sensor (possibly, a shunt resistor).

Cost Function Analyzed and Optimization Process

The cost function analyzed in the proposed control has only one main objective: to track a current reference. Thus (5),

$$u(k) = |i^*[k+1] - i_L[k+1]| \quad (3)$$

where $i(k+1)$ is the future current reference, given by the external voltage loop. The optimization process consists in to evaluate the cost function in the case with switch active and the cost with the switch inactive. The state with lower cost is chosen to be applied in the system. For example: consider that in a given instant k the current reference i^* is 5 A, $i_L(k) = 4.8$ A, $t_s = 0.1$ ms (t_s is the controller sampling time), $L = 10$ mH, $v_{in} = 70$ V and $v_{out} = 120$ V. The control will calculate the $i_L(k+1)$ using (1) and will obtain that $i_L(k+1) = 5.5$ A. After, the control will calculate $i_L(k+1)$ using (2) and will obtain that $i_L(k+1) = 4.3$ A. Using (3), the cost of to active the switch is 0.5 A and the cost of to block the switch is 0.7 A. Therefore, the controller will choose to active the switch, since this condition has lower cost.

SYSTEM DESIGN WITH PREDICTIVE CONTROLLER

Considering the presence of current predictive controller, the design methods for the converter and the voltage external loop are presented in this section.

Converter Design

Table I presents the design criteria of the simulated boost converter. A disadvantage of finite control set predictive controllers is the operation in variable switching frequency. As there is not a modulation with a fixed switching frequency, the design Of

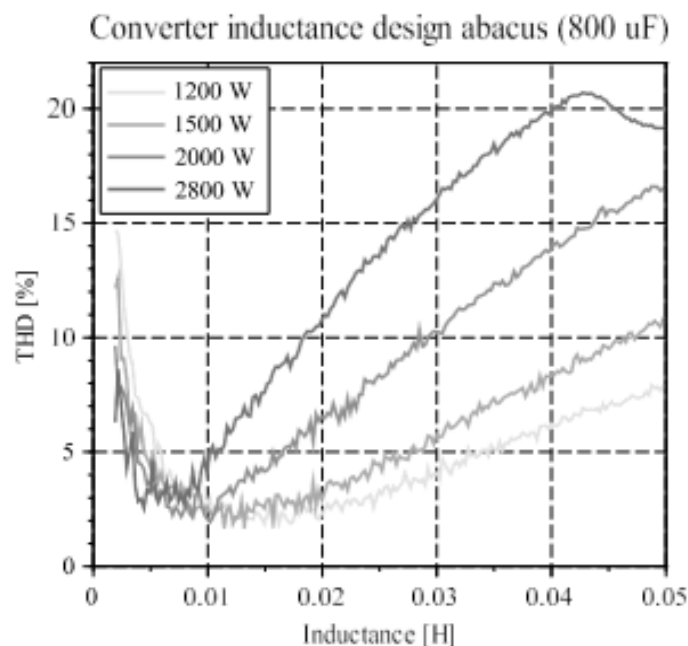


Fig. 2. Abacus for THD evaluation

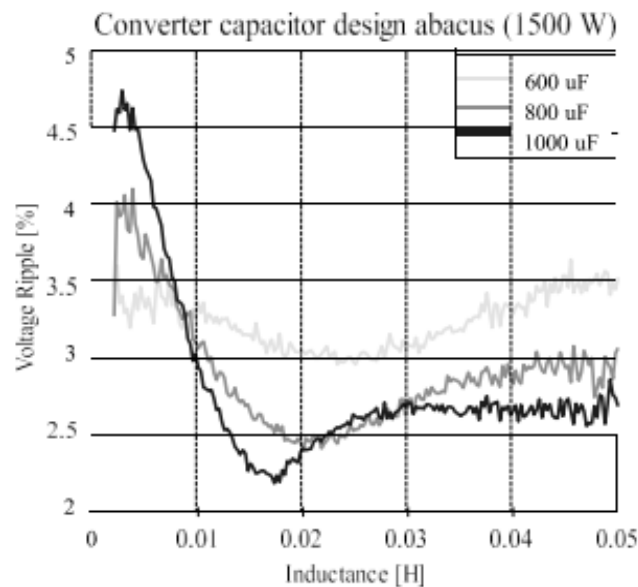


Fig. 3. Abacus for output voltage ripple evaluation

Due to this condition, an abacus was developed to help in the converter design, in terms of expect total harmonic distortion (THD) in function of inductance value and the converter power. The output capacitance has minimal influence in the curves of the abacus. Figure 2 presents the abacus for These abacus were developed as contribution of this work. In the process of the elaboration of the abacus, a current closed loop with predictive control, with a current reference as input was considered. The power curves was obtained varying the amplitude of the current reference. A sinusoidal wave (220 V) was considered as the phase input voltage in the converter. Moreover, the THD calculated considers fundamental frequency of 60 Hz (same of the input voltage). The sample time considered was 0.5 ms.

These abacus facilitate the design of the converter. The first abacus (Fig. 2) allows to choose a inductance range to reduce the THD, in function of the converter power. To determine the capacitance value, it is necessary to utilize the second abacus (Fig. 3), using the output voltage ripple as the design criteria. For this criteria, there are influences from the capacitance and the inductance. Therefore, it is possible to select the capacitance and the inductance that attends the voltage ripple criteria (obviously, respecting the THD criteria). The second abacus has low influence of the voltage converter. Logically, when there is an external voltage control loop, the THD index will have a small augment while the voltage ripple will reduce. Then, applying this methodology, it is possible to determine the passive elements of the boost converter, to apply the MPC current control. Considering the output power equals to 1500 W, the inductance values among 5 mH and 20 mH generate a THD lower than 4%, as seen in the first abacus (Fig. 2). After establish the inductance range, it is possible to analyze the second abacus (Fig. 3). In the chosen inductance range, in the curve with capacitance equals to 1000 μ F, it is possible to see that for values among 12.0 mH and 20 mH, the voltage ripple is lower than 2.5%. This the chosen values of inductance and capacitance are: $L = 14.5$ mH and $C = 1000.0$ μ F.

Voltage Loop Control Design

For voltage control loop, it is proposed to use a numerically identified model. To get this model, it is used the plant output response for a given input. With the input and the output data, a least squares algorithm can be used to obtain the model parameters (11), (14). Thus, applying this procedure, a step in current reference was applied and the voltage response was analyzed. The model is given by:

$$v_{out}[k+1] = a_g v_{out}[k] + b_g i^*[k] \quad (4)$$

where a_g and b_g are the model parameters and i^* is the current reference, in a discrete time k . This way, $a = 0.9989427$ and $b = 0.0430124$ for $t_s = 0.5$ ms. In continuous frequency (s - plane), the model is given by:

$$\frac{V(s)}{I^*(s)} = \frac{k_g}{s + p_g} \quad (5)$$

THD evaluation. Another abacus was developed to help with the converter design in relation to the output voltage ripple. It was plotted in function of inductance value, for different capacitance values and convert power values. Output power has minimal influence on the ripple curves of the abacus. Figure 3 presents the abacus for capacitor design.

with $k_g = 86.02 \text{ V/(As)}$ and $p_g = 2.11 \text{ rad/s}$. Using frequency response method, a proportional- integrative control was designed. The controller zero was placed at two times the plant pole value. The open-loop

cut-off frequency was placed at 1.0 Hz (for minimize voltage loop influence in the current THD). Therefore, the proportional gain $k_p = 0.096 \text{ A/V}$ and integrative gain $k_i = 0.404 \text{ A V}^{-1} \text{ s}^{-1}$. These gains are valid for a continuous PI controller, but, as the switching frequency is very high they were also valid for the employed digital controller. Note that the digital PI controller is given with:

$$\tilde{v}^*[k] = k_p(v^*[k] - v_{out}[k]) + k_i \sum_{\zeta=0}^k (v^*[k_\zeta] - v_{out}[k_\zeta])t_s \tag{6}$$

where v is the voltage reference and k_ζ is a counter.

SYSTEM DESIGN WITH PI CONTROLLER

In this Section, the active PFC system design is presented For the voltage control loop, it was considered the model given by:

Considering a system with two PI loops in the cascade struc

Converter Design

Considering the input v_{in} as the absolute value of a sinu- soidal curve, it is possible to define the voltage factor α as:

$$\alpha = \frac{V_{in,p}}{V_{out}} \tag{7}$$

where $V_{in,p}$ is the peak voltage of input voltage and V_{out} is the mean value of output voltage. This way, the inductance can be calculated as:

$$I = \begin{cases} \frac{V_{in,p}}{\Delta I_1 f_s} (1 - a) & \text{if } a < \text{zero.five} \\ \frac{V_{out}}{\text{four} \Delta I_1 f_s} & \text{if } a > \text{zero.five} \end{cases} \tag{8}$$

where I_L (in ampere) is the maximum current ripple. The output capacitance is given by:

$$C = \frac{P_{out}}{2\pi f V_{out} \Delta V_{out}} \tag{9}$$

Rectifier model

The full bridge diodes rectifier was modeled as an absolute value function. This way where P_{out} is the load power, f is the grid frequency and V_{out} is the output voltage ripple. Adopting the methodology above, considering $I_L = 0.5 \text{ A}$ and $V_{out} = 6 \text{ V}$, the values of $L = 10 \text{ mH}$ and $C = 1.65 \text{ mF}$ are obtained.

Control Design

For the control design, there are two schemes: internal current scheme and external voltage scheme. The internal current loop is done considering the simplified where v_{in} is the input voltage of boost converter and v_0 is instantaneous voltage of the input source.

$$\frac{\tilde{i}(s)}{d(s)} = \frac{V_{out}}{sL} \tag{10}$$

where d is the duty cycle. This model is valid for high frequency aspects and help to design the proportional gain of the controller. After that, it is just necessary a small integrative gain, to put the controller zero near to PI origin pole. This way, for a five kHz open-loop cut-off frequency, $k_{p,i} = 1.5 \text{ A}^{-1}$ and

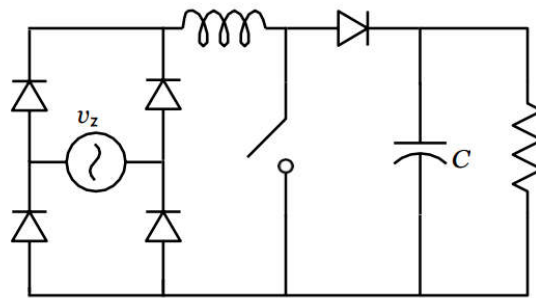
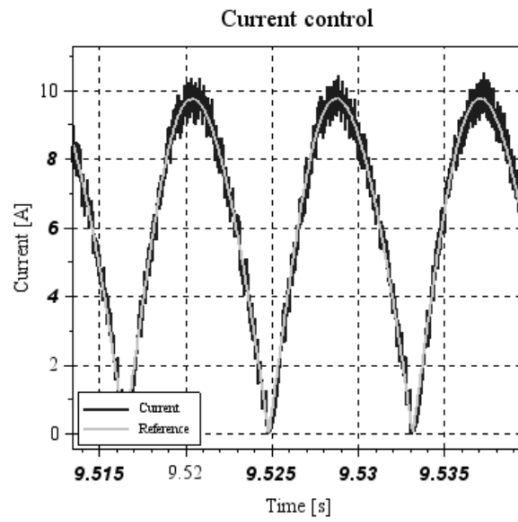


Fig. 4. Simulated Converter

$$\frac{v(s)}{i(s)} = \frac{D/C}{s + RC} \tag{11}$$

where D is the mean duty cycle value. For this model, it was established a 6 Hz open-loop cut- off frequency. The voltage controller zero is used to cancel the plant pole. Thus, $k_{p,v} = 0.15 \text{ A V}^{-1}$ and $k_{i,v} = 0.9 \text{ A}$

SYSTEM MODELING

A simulation platform was developed in C language to emulate the non controlled rectifier with boost converter for improving power factor. Figure 4 exhibits the simulated converter. Two simulation models were developed: one for the non controlled rectifier and other for the boost converter. All the system operates in closed loop. All semiconductors were considered ideal. Load disturbances were included in the

where $V_{in,p}$ is the peak voltage of input voltage and V_{out} is the mean value of output voltage.

This way, the inductance can be calculated as:

Boost converter model

The boost converter model for simulation was done using the operation stages (3). In the first stage, the switch is active, thus where d is the duty cycle. This model is valid for high frequency aspects and help to design the proportional gain of the controller. After that, it is just necessary a small integrative In the second stage, the switch is inactive, with $i_L(t) > 0$. This way, $di_L(t)$ gain, to put the controller zero near to PI origin pole. This way, for a 5 kHz open-loop cut-off frequency, $k_{p,i} = 1.5 \text{ A}^{-1}$ and full bridge diodes rectifier was modeled as an absolute value function.

$$v_{in}(t) = \begin{cases} v_{zero}(t) & \text{if } v_{zero}(t) \geq \text{zero} \\ -v_{zero}(t) & \text{if } v_{zero}(t) < \text{zero} \end{cases} \tag{12}$$

This way where v_{in} is the input voltage of step-up converter and v_{zero} is instantaneous voltage of the input source.

Step-up converter model

The step-up converter model for simulation was done using the operation stages (three).

In the first stage, the switch is active, thus

$$v_1(t) = v_{in}(t) = L \frac{di_1(t)}{dt} \tag{13}$$

$$i_C(t) = -i_{out}(t) = C \frac{dv_C}{dt} \tag{14}$$

In the second stage, the switch is inactive, with $i_1(t) > zero$.

$$v_1(t) = v_{in}(t) - v_{out}(t) = L \frac{di_1(t)}{dt} \tag{15}$$

$$i_C(t) = i_1(t) - i_{out}(t) = C \frac{dv_C}{dt} \tag{16}$$

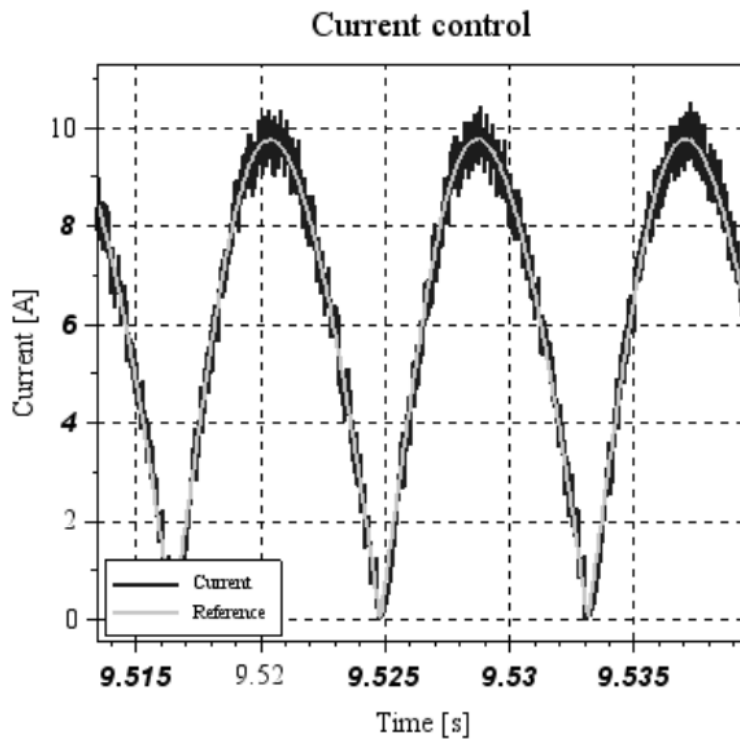


Fig. 5. Flow of electrons reference tracking with FCS-MPC

Finally, if the converter operates in a discontinuous flow of electrons mode, there is a third stage. In this stage:

$$v_1(t) = zero \tag{17}$$

$$i_1 = zero \tag{18}$$

$$i_C(t) = -i_{out}(t) = C \frac{dv_C(t)}{dt} \tag{19}$$

This way Finally, if the converter operates in a discontinuous flow of electrons mode, there is a third stage. In this stage:

Table 2. Presents a11 main parameters used in the simula tions

| Parameter | Value | Parameter | Value |
|--------------------------------|---------------------|-------------------------|------------|
| Simulation step | ten ^{-six} | <i>I</i> with MPC | 1four.five |
| Simulation total time | ten s | <i>C</i> with MPC | 1.zero |
| Simulation minimum time | nine,fiv | <i>I</i> with PI | ten.zero |
| Points evaluated | fivezer | <i>C</i> with PI | 1.sixfive |
| Control sampling time | fivezer | Output Power | 1 fivezer |
| PI switching frequency | 2zero | V_{out} | fourzero |
| MPC max. switching frequency | ten kHz | $V_{in,p}$ | three11 |
| Voltage PI (MPC) k_p | zero.zer | V. PI (MPC) k_i | zero.fou |
| Flow of electrons PI $k_{p,i}$ | 1.five | <i>C</i> . PI $k_{i,i}$ | zero.zer |
| Voltage PI $k_{p,v}$ | zero.1fi | V. PI $k_{i,v}$ | zero.nin |

SIMULATION RESULTS AND DISCUSSION

This Section presents the simulation results of both evaluated active PFC systems. In both simulations, a load disturbance is considered (reduced from tenzero% to fivezero%).

PFC with flow of electrons MPC

Figure five presents the flow of electrons reference tracking with FCS- MPC controller. Figure six presents the flow of electrons harmonics, comparing with the values established by IEC Figure seven presents command spectra using FCS-MPC for control and modulation. Figure eight presents the voltage transient with load disturbance.

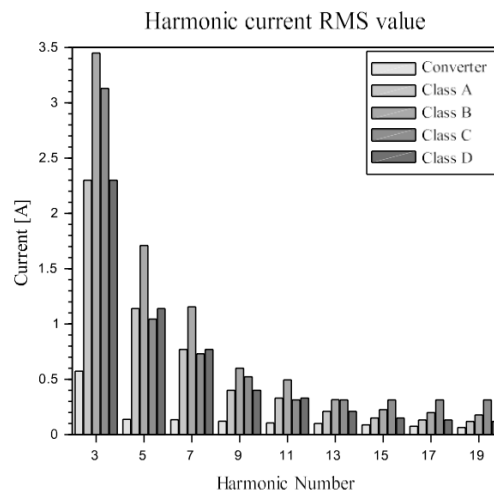


Fig. 6. Flow of electrons harmonics comparison with IEC sixtenzerozerthree-2 with FCS-MPC

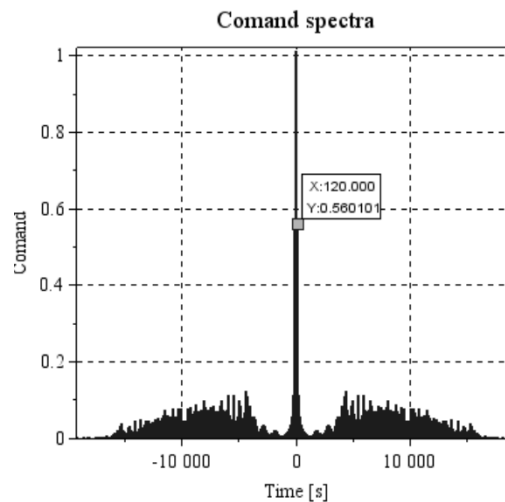


Fig. 7. Command frequency spectra with FCS-MPC

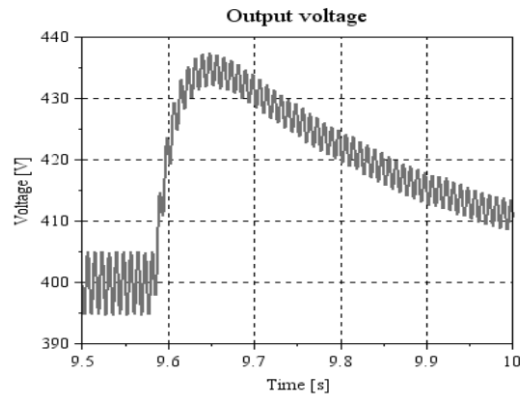


Fig. 8. Voltage transient with load disturbance with FCS-MPC in internal loop

PFC with PI controller

Figure nine presents the flow of electrons reference

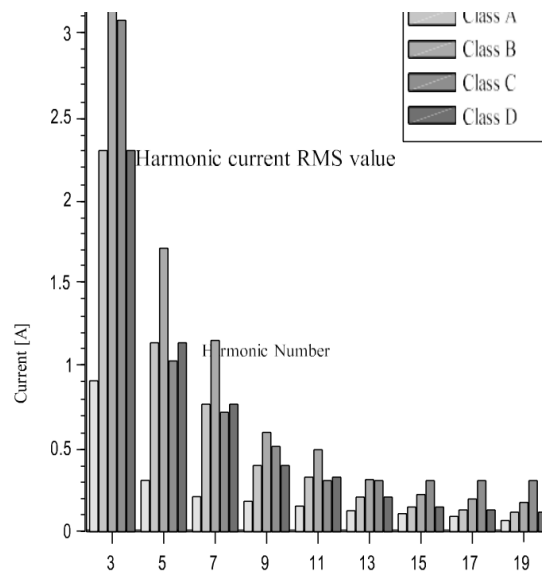


Fig. 9. Flow of electrons reference tracking with PI

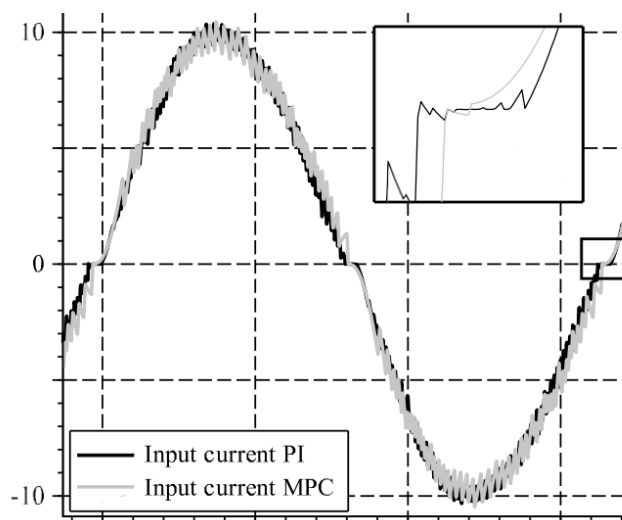


Fig. 10. Flow of electrons harmonics comparison with IEC sixtencerozero-three-2 with PI

Figure ten presents the flow of electrons harmonics, comparing with the values established by IEC

sixtenzerozero-three-2 (1). Figure 11 presents command spectra using FCS-MPC for control and modulation. Figure seven presents command spectra using FCS-MPC for control and modulation. Figure eight presents the voltage transient with load disturbance.

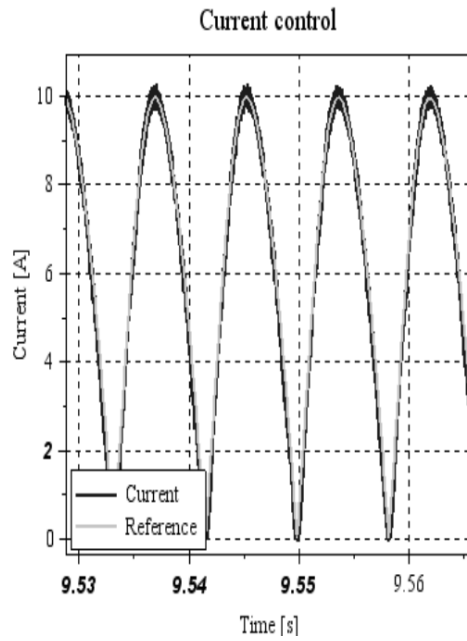


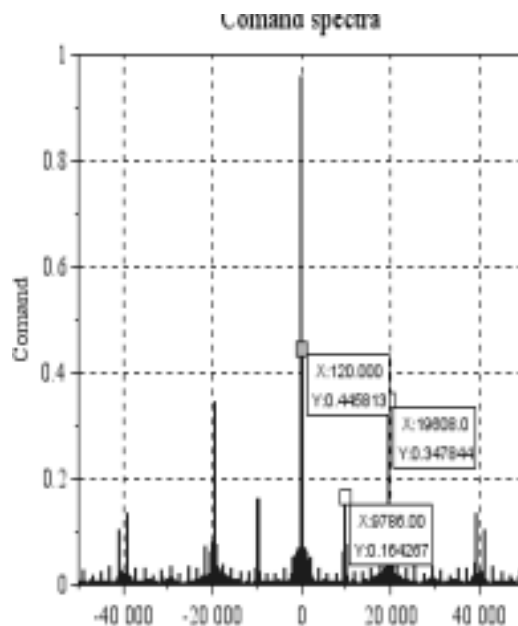
Figure 12. Presents the voltage transient with load disturbance

DISCUSSION

Table III presents the THD value for different load conditions, in steady state, comparing PI flow of electrons controller and FCS-MPC flow of electrons controller. Figure 11 presents the comparison of i_{zero} (flow of electrons on the sinusoidal source) using PI controller and using the MPC.

Fig. 11. Command frequency spectra with PI TABLE III. Thd For Different load Conditions

| load | THD with FCS-MPC | THD with PI |
|---------|------------------|----------------|
| 2zero | nine.sixfour% | 1 five.1 five% |
| fourze | four.eightseven% | nine.three2% |
| sixer | four.sevenseven% | seven.2three |
| eightz | four.1six% | six.2nine% |
| tenzero | four.zeroseven% | six.zerosix% |
| 12zero | four.threesix% | six.2six% |



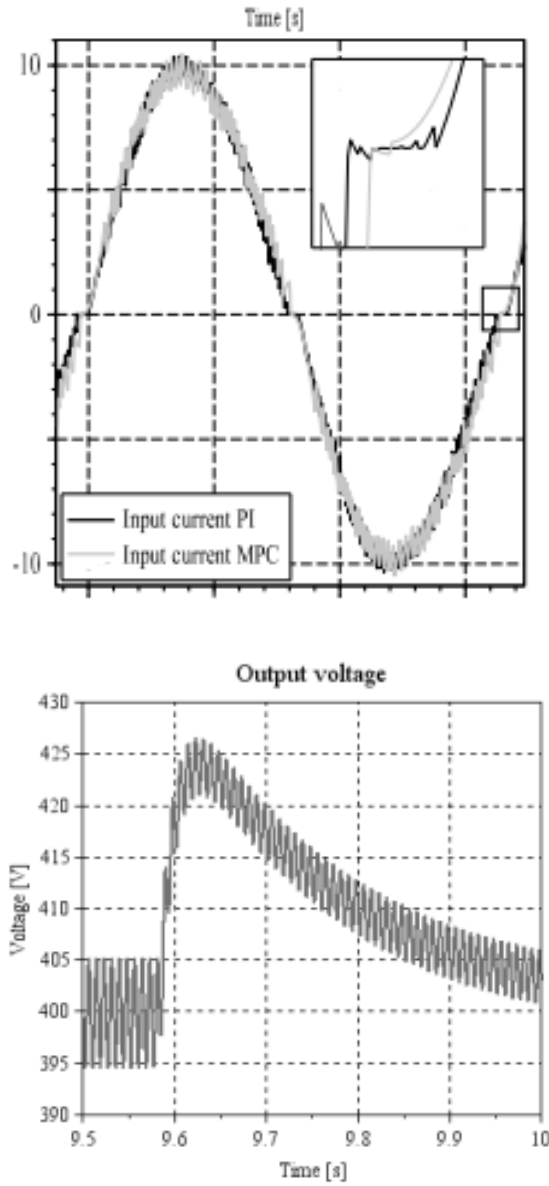


Fig. 12. Voltage transient with load disturbance with PI in internal loop

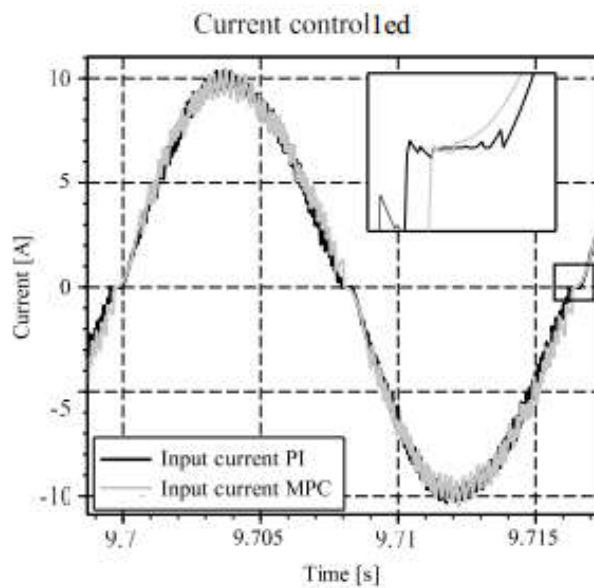


Fig. 13. Source flow of electrons comparison (zero crossover in detail)

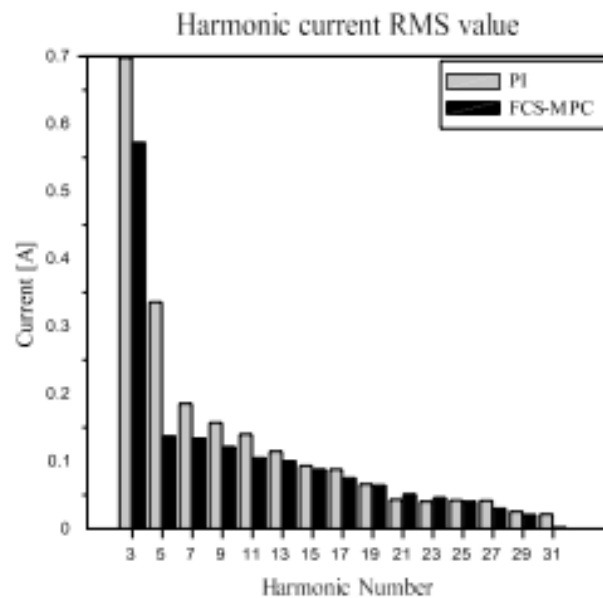


Fig. 14. Harmonic flow of electrons comparison between PI controller and MPC

In detail, the zero crossover is shown. Figure 14 exhibits the comparison of i_{zero} harmonics between PI controller and MPC. Both active PFC fulfilled the norm, as seen in Fig. six and Fig. ten (even in higher harmonics that are not seen in these figures). However, there are some peculiarities that needs highlights:

- Besides the PFC design with MPC were made for THD = three%, the obtained result at rated operation can be considered satisfactory (see Table III). Obviously, there is some distortion in the own flow of electrons reference, since there is some influence of voltage loop. Considering only the flow of electrons loop, the results are agreeing with the project.
- The same occurs with project for PFC with PI flow of electrons control: the external voltage loop reduces the quality of the results, although the result still is in agreement with the international standard.
- Compared directly one with other (Fig. 14), MPC presented lower harmonic flow of electrons amplitude for low harmonics while PI had some lower harmonic flow of electrons amplitude for some of high harmonics. Overall, MPC had lower individual harmonics, which explains the lower THD than the PI.
- The voltage loop with PI flow of electrons controller in internal loop is faster than the voltage loop with MPC flow of electrons controller in internal loop. This way, in the load disturbance, the first had lower voltage peak (six, five% – see Fig. 12) than the second (nine, zero% – see Fig. eight). To improve this results, it is necessary to use a higher cut-off frequency in the control design. However, as faster the voltage loop is, worst the flow of electrons THD will be. Note that the voltage ripple,
- in both conditions were the same (1.2 five%), as predicted in converter design (both converters were designed for 1. five-2. zero% voltage ripple).
- Analyzing Fig. seven and Fig. 11, the fundamental frequency of command signal (despite the DC level) is the 12 zero Hz, used to tracking the flow of electrons reference (see Fig. five and Fig. nine). However, in the PI command, frequencies at almost ten kHz and 2 zero kHz are distinct in the harmonic spectra, since there are a fixed operation frequency. In the MPC command, operation frequency is limited to 2 zero kHz of sampling frequency, but it is a variable frequency. Therefore, this control acts in the frequency it needs to act at each moment. It is interesting that the frequency grows to track the peak of the flow of electrons reference and reduces to track the reference in low values.
- The flow of electrons ripple with PI flow of electrons controller is considerably lower than with the MPC flow of electrons controller. Since PI operates in a high fixed frequency, the inductor is capable to filter the higher harmonics caused by switching frequency. As the MPC frequency is lower, the flow of electrons ripple is higher since the inductor do not filter these low frequencies. Otherwise, in the converter design with PI flow of electrons controller, the inductor was designed considering the flow of electrons ripple. In the converter design with MPC flow of electrons controller, the inductor was designed considering the input flow of electrons THD. It explains why the MPC has lower THD even with higher flow of electrons ripple. Notably, in the zero point of the reference, with PI flow of electrons controller, there is a flow of electrons dead zone, which also reduces the THD. With MPC controller tracking the reference, this effect is attenuated, which improves the THD (as seen in
- Fig. 13).
- The step-up converter with MPC flow of electrons control used a lower output filter for the same voltage ripple. In other hand, the step-up converter with PI used a lower inductance than the MPC and gives lower flow of electrons ripple, besides the higher THD.
- Both controllers presented lower THD even in low load condition. It explains the advantage of active PFC in relation to passive PFC, independently of the employed technique

Conclusion

This work presented a design methodology for active PFC with FCS-MPC flow of electrons controller. The design was evaluated and compared with a conventional PI flow of electrons controller solution for active PFC with boost converter. The presented design methodology uses 2 abacus for design the inductance and the capacitance of step-up converter, considering a predictive flow of electrons control. For voltage control design, the use of a numerically identified model was considered. The methodology shows itself valid, since the final THD was near to expected in the project. The comparison with PI controller showed the differences between both techniques. As PI operates with fixed switching frequency, the flow of electrons ripple with this technique is lower, but it is incapable to lead with zero points of flow of electrons reference which reduced its THD (associated to this fact is the faster voltage loop, which causes some distortion in flow of electrons reference). This way, the predictive controller presented lower THD, at rated operation and in any other tested load condition if compared with PI. The active PFC techniques are a reliable solution for equipment with non controlled rectifiers in input stage and need to fulfill international standards. The presented techniques were capable to fulfilled the IEC sixteenzerozero three-2 standard and have high power factor, allowing better use of industrial electric grids, with these equipment. For futures works, it is suggested to explore FCS-MPC with higher prediction horizons, to compare the finite control set technique with continuous control set MPC techniques and to test the capability of MPC techniques in constrainttreatment.

REFERENCES

- (1) *Electromagnetic compatibility (EMC) Part three-2: Limits - Limits for harmonic flow of electrons emissions (equipment input flow of electrons ≤ 16 A per phase)*, IECsixteenzerozero-three-2 Std., 2zerozerofive.
- (2) I. Roggia, J. E. Baggio, and J. R. Pinheiro, "Predictive flow of electrons controller for a power factor correction step-up converter operating in mixed conduction mode," in *13th European Conference on Power Electronics and Applications*, 2zerozeronine. *EPE zeronine.*, 2zerozeronine, pp. 1–ten.
- (3) Wall, S. and Jackson, R. "Fast controller design for single-phase power-factor correction systems," *IEEE Transactions on Industrial Electronics*, vol. fourfour, no. five, pp. sixfivefour–sixsixzero, Oct 1ninenine.
- (4) I. Roggia, F. Beltrame, J. E. Baggio, and J. R. Pinheiro, "Digital flow of electrons controllers applied to the boost power factor correction converter with load variation," *IET Power Electronics*, vol. five, no. five, pp. fivethree2 – fivefour1, 2zero12.
- (5) Vazquez, S., Leon, J. I. Franquelo, J. Rodriguez, H. Young, A. Marquez, and P. Zanchetta, "Model predictive control: A review of its applications in power electronics," *IEEE Industrial Electronics Magazine*, vol. eight, no. 1, pp. 1six–three1, Marc ,o 2zero1four.
- (6) Bouafassa, A. I. Rahmani, B. Babes, and R. Bayindir, "Experimental design of a finite state model predictive control for improving power factor of boost rectifier," in *2zero1five IEEE 15th International Conference on Environment and Electrical Engineering (EEEIC)*, 2zero1five, pp. 1fivefivesix – 1fivesix1.
- (7) Bordons, C. and C. Montero, "Basic principles of mpc for power converters: Bridging the gap between theory and practice," *IEEE Industrial Electronics Magazine*, vol. nine, no. three, pp. three1– fourthree, Setembro 2zero1five.
- (8) Geng, Y. Y. Liu, J. Chen, and P. Luo, "Analysis and design of a predictive ccm power factor correction converter," in *2zero1three International Conference on Communications, Circuits and Systems (ICCCAS)*, 2zero1three, pp. threenineeight – fourzero1.
- (9) Abedi, M., Song, B.M. and Erzen, B. "Optimum tracking of nonlinear-model predictive control for boost based pfc rectifier," in *2zero11 IEEE fourtheerd Southeastern Symposium on System Theory*, 2zero11, pp. eightseven–nine1.
- (10) Yazdani, M., Farhangi, S. and Zolghadri, M. R. "A novel control strategy for power factor corrections based on predictive algorithm," in *2zeroten 1st Power Electronic & Drive Systems & Technologies Conference (PEDSTC)*, 2zeroten, pp. 11seven–121.
- (11) Qin, S. J. and Badgwell, T. A. "A survey of industrial model predictive control technology," *Control Engineering Practice*, vol. 11, pp. seventhreethree–sevensixfour, 2zerozerothree.
- (12) Mayne, D. Q. "Model predictive control: Recent developments and future promise," *Automatica*, vol. fivezero, pp. 2ninesixseven– 2nineightsix, November 2zero1four.
- (13) Young, H., Perez, M., Rodriguez, J. and Abu-Rub, H. "Assessing finite-control-set model predictive control," *IEEE Industrial Electronics Magazine*, vol. eight, no. 1, pp. fourfour–five2, March 2zero1four.
- (14) Negri, G., Bartsch, M., A.G. and Cavalca, J. de Oliveira, A. Nied, and A. Silveira, "Model-based predictive direct speed control applied to a permanent magnet synchronous motor with trapezoidal back-emf," in *2zero1four 11th IEEE/IAS International Conference on Industry Applications (INDUSCON)*, 2zero1four.
